IEEE Access
Multidisciplinary | Rapid Review | Open Access Journal

Date of publication xxxx 00, 0000, date of current version xxxx 00, 0000.

Digital Object Identifier 10.1109/ACCESS.2017.DOI

Sensorless Tracking Control for a "Full-Bridge Buck Inverter–DC Motor" System: Passivity and Flatness-Based Design

RAMÓN SILVA-ORTIGOZA[1], EDUARDO HERNÁNDEZ-MÁRQUEZ[2], ALFREDO ROLDÁN-CABALLERO[1], SALVADOR TAVERA-MOSQUEDA[1], MAGDALENA MARCIANO-MELCHOR[1], JOSÉ RAFAEL GARCÍA-SÁNCHEZ[3], VICTOR MANUEL HERNÁNDEZ-GUZMÁN[4], AND GILBERTO SILVA-ORTIGOZA[5]

[1]Instituto Politécnico Nacional, CIDETEC, Laboratorio de Mecatrónica y Energía Renovable, C.P. 07700, Mexico City, México
[2]Tecnológico Nacional de México, Instituto Tecnológico Superior de Poza Rica, Departamento de Ingeniería Mecatrónica, C.P. 93230, Veracruz, México
[3]Tecnológico Nacional de México, Tecnológico de Estudios Superiores de Huixquilucan, División de Ingeniería Mecatrónica, C.P. 52773, Estado de México, México
[4]Universidad Autónoma de Querétaro, Facultad de Ingeniería, Centro Universitario, C.P. 76010, Querétaro, Qro., México
[5]Benemérita Universidad Autónoma de Puebla, Facultad de Ciencias Físico Matemáticas, C.P. 72570, Puebla, Pue., México

Corresponding author: Ramón Silva-Ortigoza (rsilvao@ipn.mx)

This work was supported by the Instituto Politécnico Nacional, México. The work of R. Silva-Ortigoza and M. Marciano-Melchor was supported by the SNI-México and IPN programs EDI and SIBE. The work of E. Hernández-Márquez, J. R. García-Sánchez, V. M. Hernández-Guzmán, and G. Silva-Ortigoza was supported by the SNI-México. The work of A. Roldán-Caballero and S. Tavera-Mosqueda was supported by the CONACYT-México and BEIFI scholarships.

ABSTRACT A sensorless control based on the exact tracking error dynamics passive output feedback (ETEDPOF) methodology is proposed for executing the angular velocity trajectory tracking task on the "full-bridge Buck inverter–DC motor" system. When such a methodology is applied to the system, the tracking task is achieved by considering only the current sensing and by using some reference trajectories for the system. The reference trajectories are obtained by exploiting the flatness property associated with the mathematical model of the "full-bridge Buck inverter–DC motor" system. Experimental tests are developed for different desired angular velocity trajectories. With the aim of obtaining the experimental results in closed-loop, a "full-bridge Buck inverter–DC motor" prototype, Matlab-Simulink, and a DS1104 board from dSPACE are employed. The experimental results show the effectiveness of the proposed control.

INDEX TERMS Motor drivers, power converters, full-bridge Buck inverter, DC motor, passivity control, differential flatness, trajectory tracking.

I. INTRODUCTION

Permanent magnet DC motors are used in a wide range of applications [1]. Such applications, for mentioning a few, are: domestic life (kitchen equipment, washing machines, toys, cameras, etc.), public life (autobank machines, automatic vending machines, ticketing machines, etc.), and industry (industrial drives, machine tools, robots, etc.). From those applications, and with the aim of achieving a better performance in DC motors, in the last years these systems have been intensively studied by the automatic control community. In that direction, in the last decade, different topologies of DC/DC power electronics converters have been used as drivers for DC motors. One of those topologies is the DC/DC Buck power electronic converter. This topology has been extensively used as a driver for DC motors; the most relevant contributions regarding the latter has been reported in [2]–[34]. Such contributions can be classified in "SISO DC/DC Buck converter–DC motor" [2]–[30] and "MIMO DC/DC Buck converter–inverter–DC motor" [31]–[34] for unidirectional and bidirectional movement, respectively. The unidirectional movement is related to the clockwise rotation of the motor shaft, while the bidirectional one implies both, the clockwise and the counter-clockwise rotation of the motor shaft. Meanwhile, important contributions related to other

This article has been accepted for publication in a future issue of this journal, but has not been fully edited. Content may change prior to final publication. Citation information: DOI 10.1109/ACCESS.2021.3112575, IEEE Access

DC/DC converters used as drivers for DC motors have been reported in [35] and [36] (for multilevel and parallel Buck topologies, respectively), [37]–[44] (for Boost topology), [45]–[50] (for Buck-Boost topology), [51] (for Sepic topology), [52] (for Luo topology), and [53] (for Cuk topology). In the following, the "SISO DC/DC Buck converter–DC motor" and the "MIMO DC/DC Buck converter–inverter–DC motor" contributions reported in literature are presented.

A. "SISO DC/DC BUCK CONVERTER–DC MOTOR" SYSTEM

For the first time, in 2000 Lyshevski developed the mathematical model and a nonlinear PI control for the angular velocity regulation task for the DC/DC Buck converter–DC motor system [2]. Later, in 2010 Ahmad *et al.* in [3] analyzed a comparative assessment of the PI, fuzzy PI, and LQR control strategies for the velocity of the motor. In 2012, Bingöl and Paçaci in [4] used a virtual laboratory based on neural networks for controlling the angular velocity of the system. A year later, in 2013 a robust control based on active disturbance rejection and differential flatness for two configurations of the Buck converter–DC motor system was addressed by Sira-Ramírez and Oliver-Salazar in [5]. Whereas Hoyos *et al.* in [6]–[9] studied the zero average dynamics and fixed-point induced control for the motor speed of a Buck converter and DC motor coupled system. By exploiting the flatness of the system, for the angular velocity tracking task, Silva-Ortigoza *et al.* explained two hierarchical robust controls; in 2013 a sensorless control approach based on integral reconstructors [10] and in 2014 the experimental verification of a hierarchical control based on flatness [11]. An adaptive robust control based on dynamic surface control and sliding mode control (SMC) was exhibited by Wei *et al.* [12]. In 2015, Silva-Ortigoza *et al.* exposed a hierarchical controller composed of two independent controls; one via differential flatness (for the DC motor) and the other one via a cascade scheme through SMC and PI control (for the Buck converter), which were interconnected in order to work as a whole [13]. A control based on the exact tracking error dynamics passive output feedback (ETEDPOF) methodology was presented by Srinivasan and Srinivasan in [14]. Additionally, Hernández-Guzmán *et al.* in [15] introduced a SMC with PI controls to regulate the converter capacitor voltage, the motor armature current, and the motor velocity. Later, in 2016 Khubalkar *et al.* in [16] utilized a fractional order PID control whose tuning was executed with the dynamic particle swarm optimization (dPSO) technique. Rigatos *et al.* in [17] reported a control based on the differential flatness theory and used a derivative-free nonlinear Kalman filter for compensating disturbances. Another solution was implemented in 2017 by Nizami *et al.* in [18], where a neuro-adaptive backstepping control method, using a single-layer Chebyshev polynomial based neural network, was exposed. In 2018, Rigatos *et al.* in [19] provided a flatness-based control in successive loops for the tracking task. Meanwhile, Khubalkar *et al.* in [20] applied a fractional order PID control with an improved dSPO technique. Recently in 2019, Yang *et al.* in [21] designed a discrete-time robust predictive speed regulation algorithm by using a discrete-time reduced-order generalized proportional-integral (GPI) observer. Likewise, Hanif *et al.* in [22] proposed a piecewise affine PI control based on the safe experimentation dynamics algorithm. While Kazemi and Montazeri in [23] showed a fault detection system using a combination of bond graph method and a switching observer. More recently, in 2020 an H-infinity adaptive neurofuzzy control method was exploited by Rigatos *et al.* in [24]. Whereas Rauf *et al.* in [25] elaborated a continuous dynamic sliding mode control with high order mismatched disturbance compensation. Additionally, Srinivasan *et al.* in [26] introduced a sensitivity analysis for the ETEDPOF methodology applied to the DC/DC Buck converter–DC motor system. Lastly, the important problem of active disturbance rejection control was also tackled by Stanković *et al.* in [27] and Madonski *et al.* in [28] for harmonic disturbances and multiple uncertainties, where resonant extended observers were utilized. Other interesting papers, recently published, associated with the connection of the DC/DC Buck power converter and DC motor have been reported in [29] and [30].

B. "MIMO DC/DC BUCK CONVERTER–INVERTER–DC MOTOR" SYSTEM

In recent years, Silva-Ortigoza *et al.* described the development and experimental validation of a mathematical model associated with the DC/DC Buck converter–inverter–DC motor system [31]. Likewise, the design of a control based on the ETEDPOF methodology for the bidirectional angular velocity tracking of the system was considered in [32]. Later, Hernández-Márquez *et al.* in [33] employed two robust controls based on flatness for solving the angular velocity tracking task of the DC/DC Buck–inverter–DC motor system. Lastly, a control based on the adaptive sliding mode technique with neural network estimation for the bidirectional DC motor system consisting of a DC/DC Buck converter, a full bridge inverter, and a DC motor was investigated by Chi *et al.* in [34].

C. DISCUSSION OF RELATED WORK, MOTIVATION, AND CONTRIBUTION

During the last years, different control strategies for driving a DC motor fed via DC/DC Buck power converters have been proposed. Related to such contributions the following was found:

- For the "SISO DC/DC Buck converter–DC motor" system [2]–[30], the angular velocity control is unidirectional. This latter, because the output voltage of the Buck converter is unipolar. Some applications that have been profited, although some kind limited, from using this system can be found in mechatronic systems [54], robotic arms [55], and wheeled mobile robots [56]–[58].
- By using the "MIMO DC/DC Buck converter–inverter–DC motor" system [31]–[34] the unidirectional rotation

restriction associated with the DC motor shaft is overcome, since an inverter circuit is introduced between the Buck converter and the DC motor. An application recently developed that uses such a system can be found in [34], where the problem of renewable energy power source based on fuel cells was presented by Chi *et al.* in 2020.

Motivated by the benefits of the new "full-bridge Buck inverter–DC motor" system [59]:

- On the one hand, this kind of system is a linear SISO system, and at the same time, that drives bipolar voltage to the DC motor. In consequence, and unlike the contributions presented so far for the "SISO DC/DC Buck converter–DC motor" system in [2]–[30], this is the manner to overcome the unidirectional rotation limitation associated with the DC motor shaft.
- On the other hand, the mathematical model of such a system exhibits a special "energy managing" structure [60], [61], which is naturally suited for the ETEDPOF controller design methodology. This control strategy was studied initially by Sira-Ramírez (see the seminal work of Sira-Ramírez [60] for the underlying theoretical considerations and see [61] for the potential of this technique in applications). Among the numerous applications in automatic control that have been developed regarding the ETEDPOF technique, one can find those associated with traditional power electronics [61], DC motors driven by DC/DC power converters [14], [26], [32], [37], [43], [48], [51], [52], single phase active rectifiers [62], three-phase Boost rectifiers [63], airships [64], mobile robotics [65], renewable energy systems [66], separately excited DC motors [67], induction motor powered by photovoltaic panels [68], transformerless multilevel active monophase rectifiers [69], permanent magnet synchronous motors [70], and magnetorheological automotive suspensions [71].

Thus, inspired by the control applications based on the ETEDPOF methodology, in this paper a sensorless passivity-based control that considers the ETEDPOF strategy and flatness is proposed for the new "full-bridge Buck inverter–DC motor" system. Also, it is worth noting that the study of this system could lead to a favorable impact, giving rise to a new research topic, in renewable energy [34], mechatronic systems [54], robotic arms [55], wheeled mobile robots [56]–[58], [72], permanent magnet synchronous motors [73], induction motors [74], and underactuated systems [75]–[79].

From the aforementioned discussion of the state-of-the-art and motivation of the work, the main contributions of this study can be summarized as follows:

1) To design a sensorless passivity-based control by using the ETEDPOF methodology for solving the angular velocity trajectory tracking task for the new "full-bridge Buck inverter–DC motor" system.
2) To obtain the reference trajectories for the "full-bridge Buck inverter–DC motor" system. The implementation of the proposed control, via the ETEDPOF methodology, requires some reference trajectories. Such reference trajectories are generated through the differential flatness concept, since the mathematical model of the system enjoys the flatness property.
3) To experimentally verify the performance of the control, designed via the ETEDPOF methodology and the flatness concept, for different types of desired angular velocity trajectories. For this aim, a built prototype of the "full-bridge Buck inverter–DC motor" system, Matlab-Simulink, and a DS1104 board from dSPACE are used.
4) To accomplish a revision of the experimental closed-loop tracking errors, that are acquired after implementing the proposed ETEDPOF control on the system, and the experimental open-loop tracking errors (obtained in [59]). Such a revision is carried out with the intention of showing how the system in closed-loop is benefited from the ETEDPOF strategy, rather than for comparative purposes.

The remaining part of this paper is organized as follows: Section II provides a brief introduction to the "full-bridge Buck inverter–DC motor" system. Section III presents the design of the passive control via ETEDPOF for solving the trajectory tracking task on the system. The reference trajectories of the system are obtained by exploiting the flatness property and are presented in Section IV. Then, Section V discusses the experimental implementation of the proposed control and also presents the experimental validation of its performance. Finally, the paper is concluded in Section VI.

II. A NEW "FULL-BRIDGE BUCK INVERTER–DC MOTOR" SYSTEM

The electric circuit of the full-bridge Buck inverter–DC motor system is shown in Fig. 1. Such a circuit can be divided in two systems: The *full bridge Buck inverter* modulates and supplies bipolar voltage v to the DC motor via the input u. It comprises a power supply E and an array of four transistors, denoted by Q_1, $\overline{Q}_1$, Q_2, and $\overline{Q}_2$ that operates according to the clock cycles depicted in Fig. 1. In addition, the first subsystem is composed of an LC filter; where the current i flows through the inductor L and the voltage v appears over the terminals of capacitor C that is connected in parallel to the load R. The *DC motor* corresponds to the system actuator, and is made up of the following elements: R_a, L_a, and i_a, corresponding to the armature resistance, armature inductance, and armature current, respectively. Whereas ω is the angular velocity of the motor shaft. Other important parameters of the motor are J, b, k_e, and k_m, corresponding to the moment of inertia of the rotor and motor load, the viscous friction coefficient of the motor, the counterelectromotive force constant, and the motor torque constant, respectively.

According to [59], the average mathematical model of the full-bridge Buck inverter–DC motor system shown in Fig. 1

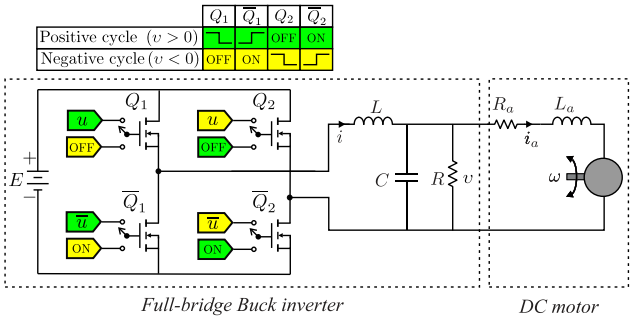

FIGURE 1. Full-bridge Buck inverter–DC motor system and clock cycles u associated with Q_1, $\overline{Q}_1$, Q_2, and $\overline{Q}_2$, for the positive cycle $(v > 0)$ and the negative cycle $(v < 0)$.

is given by,

$$\begin{aligned} L\frac{di}{dt} &= -v + Eu_{av}, \\ C\frac{dv}{dt} &= i - \frac{v}{R} - i_a, \\ L_a\frac{di_a}{dt} &= v - R_a i_a - k_e\omega, \\ J\frac{d\omega}{dt} &= k_m i_a - b\omega, \end{aligned} \tag{1}$$

with $u_{av} \in [-1, 1]$, being u_{av} the duty cycle or average input signal of the system. Whereas the rest of the variables and constants related to the mathematical model (1) were previously defined.

III. DESIGN OF THE PASSIVE CONTROL VIA ETEDPOF

This section presents the design of a passivity-based control for solving the trajectory tracking task on the full-bridge Buck inverter–DC motor system. Such a control is based on the ETEDPOF strategy, whose underlying theoretical considerations were presented in [60]. Whereas some applications of this strategy in connection with traditional power electronics were carried out in [61].

A. ETEDPOF CONTROLLER DESIGN METHODOLOGY

By invoking the seminal work of Sira-Ramírez [60], the derivation of the ETEDPOF methodology will be given here in a general setting for a better understanding. Thus, with the aim of applying such a strategy, the following convenient representation for a system is used,

$$\mathcal{A}\dot{x} = [\mathcal{J}(u_{av}) - \mathcal{R}]x + \mathcal{B}u_{av} + \eta(t), \tag{2}$$

being $\mathcal{J}(u_{av})$, for all u_{av}, of the form,

$$\mathcal{J}\left(u_{av}\right) = \mathcal{J}_0 + \sum_{i=1}^{m} \mathcal{J}_i u_{i_{av}}, \tag{3}$$

where $\mathcal{A}^{n\times n}$ is a symmetric, positive definite, constant, matrix, $\mathcal{J}(u_{av})^{n\times n}$ is a skew symmetric matrix (the matrices $\mathcal{J}_0$ and $\mathcal{J}_i$, $i = 1, \ldots, m$, are constant and skew symmetric matrices), $\mathcal{R}^{n\times n}$ is a symmetric, positive semi-definite constant matrix, $x^{n\times 1}$ is the state vector of the system, $\mathcal{B}^{n\times m}$ is a constant matrix, $u_{av}^{m\times 1}$ is the average control input vector (each component $u_{i_{av}}$ takes values on the closed interval $[-1, 1]$ of the real line), and $\eta(t)^{n\times 1}$ is a smooth vector function of time t or, sometimes, a vector of constant entries.

From (2), the desired dynamics of the system is represented as follows:

$$\mathcal{A}\dot{x}^* = [\mathcal{J}(u_{av}^*) - \mathcal{R}]x^* + \mathcal{B}u_{av}^* + \eta(t), \tag{4}$$

with

$$\mathcal{J}\left(u_{av}^*\right) = \mathcal{J}_0 + \sum_{i=1}^{m} \mathcal{J}_i u_{i_{av}}^*, \tag{5}$$

where x^* and u_{av}^* are the desired state vector and the desired average control input vector, respectively.

Defining the state error and average control error as:

$$e = x - x^*, \qquad e_{u_{av}} = u_{av} - u_{av}^*. \tag{6}$$

By subtracting (4) from (2), and after using (6), it is obtained:

$$\mathcal{A}\dot{e} = \left[\mathcal{J}\left(u_{av}\right) - \mathcal{R}\right] e + \mathcal{B}e_{u_{av}} + \left[\mathcal{J}\left(u_{av}\right) - \mathcal{J}\left(u_{av}^*\right)\right] x^*. \tag{7}$$

Now, by replacing (3) and (5) into (7) the following is obtained:

$$\begin{aligned} \mathcal{A}\dot{e} &= \left[\mathcal{J}\left(u_{av}\right) - \mathcal{R}\right] e + \mathcal{B}e_{u_{av}} + \left(\sum_{i=1}^{m} \mathcal{J}_i e_{u_{i_{av}}}\right) x^* \\ &= \left[\mathcal{J}\left(u_{av}\right) - \mathcal{R}\right] e + \underbrace{\left[\mathcal{B} + \left(\mathcal{J}_1 x^*, \ldots, \mathcal{J}_m x^*\right)\right]}_{=:\mathcal{B}^*} e_{u_{av}}. \end{aligned} \tag{8}$$

Then, the exact open-loop tracking error dynamics is given by,

$$\mathcal{A}\dot{e} = [\mathcal{J}(u_{av}) - \mathcal{R}]e + \mathcal{B}^* e_{u_{av}}. \tag{9}$$

According to the ETEDPOF methodology [61], the control $e_{u_{av}}$ that achieves $e \to 0$ is determined by,

$$e_{u_{av}} = -\Gamma \mathcal{B}^{*T} e, \tag{10}$$

being $\Gamma = \text{diag}[\gamma_1, \gamma_2, \ldots, \gamma_m] > 0$. Thus, the closed-loop tracking error dynamics, that is obtained after replacing (10) into (9), is:

$$\mathcal{A}\dot{e} = [\mathcal{J}(u_{av}) - \mathcal{R}]e - \mathcal{B}^*\Gamma\mathcal{B}^{*T} e. \tag{11}$$

In order to assess the stability of the closed-loop dynamics (11), the following positive definite Lyapunov function is proposed,

$$V(e) = \frac{1}{2} e^T \mathcal{A} e. \tag{12}$$

The time derivative of such a positive definite function, along the controlled trajectories of the tracking error dynamics, yields

$$\dot{V}(e) = e^T \mathcal{A}\dot{e} = -e^T \left[\mathcal{R} + \mathcal{B}^*\Gamma\mathcal{B}^{*T}\right] e,$$

which guaranties that $e \to 0$ as long as,

$$\mathcal{R} + \mathcal{B}^*\Gamma\mathcal{B}^{*T} > 0. \tag{13}$$

This article has been accepted for publication in a future issue of this journal, but has not been fully edited. Content may change prior to final publication. Citation information: DOI 10.1109/ACCESS.2021.3112575, IEEE Access

B. VELOCITY-SENSORLESS TRACKING CONTROL FOR THE FULL-BRIDGE BUCK INVERTER–DC MOTOR SYSTEM

After applying the previous results to the full-bridge Buck inverter–DC motor system, the following is obtained:

- First, it is verified that the average model (1) can be represented by means of the energy managing structure (2). For this, by simple inspection it is found that,

$$\mathcal{A} = \text{diag}\left[L, C, L_a, J\right], \quad \mathcal{R} = \text{diag}\left[0, \frac{1}{R}, R_a, b\right],$$

$$\mathcal{J}(u_{av}) = \begin{bmatrix} 0 & -1 & 0 & 0 \\ 1 & 0 & -1 & 0 \\ 0 & 1 & 0 & -k_e \\ 0 & 0 & k_m & 0 \end{bmatrix}, \ \mathcal{B} = \begin{bmatrix} E \\ 0 \\ 0 \\ 0 \end{bmatrix}, \ \eta = \begin{bmatrix} 0 \\ 0 \\ 0 \\ 0 \end{bmatrix},$$

$$x = [i, \upsilon, i_a, \omega]^T, \qquad x^* = [i^*, \upsilon^*, i_a^*, \omega^*]^T,$$

  where $\mathcal{J}(u_{av})$ complies with being a skew symmetric matrix, due to $k_m = k_e$ in a DC motor [80]. Whereas x^*, as previously mentioned, corresponds to the desired state vector of the system. It is worth mentioning that, for the system under study, x^* is composed of i^*, υ^*, i_a^*, and ω^* representing the desired reference trajectories associated with i, υ, i_a, and ω, respectively.
- Second, it must be verified that condition (13) is satisfied. For this, after finding $\mathcal{R}+\mathcal{B}^*\Gamma\mathcal{B}^{*T}$ and by invoking the Sylvester criterion [81] it is shown that,

$$\mathcal{R} + \mathcal{B}^*\Gamma\mathcal{B}^{*T} = \begin{bmatrix} E^2\gamma_1 & 0 & 0 & 0 \\ 0 & \frac{1}{R} & 0 & 0 \\ 0 & 0 & R_a & 0 \\ 0 & 0 & 0 & b \end{bmatrix} > 0,$$

  with $\gamma_1 > 0$. In this manner, it is concluded that the closed-loop system is asymptotically stable.
- Lastly, after verifying the previous two items and by considering (6) and (10), it is concluded that the proposed ETEDPOF control that solves the trajectory tracking task for the full-bridge Buck inverter–DC motor system is determined by,

$$u_{av} = -\gamma_1 E(i - i^*) + u_{av}^*. \tag{14}$$

  The reference trajectories i^* and u_{av}^* will be obtained from exploiting the differential flatness property enjoyed by the system (1).

C. ADVANTAGES AND LIMITATIONS OF THE ETEDPOF CONTROLLER

Having designed the passivity-based control by using the ETEDPOF strategy for solving the trajectory tracking task in the full-bridge Buck inverter–DC motor system, now it is convenient to highlight the advantages and limitations of such a strategy. In this regard, the following are considered to be advantages:

- The control (14) requires only the measurement of the converter current, i, and the knowledge of the reference trajectories i^* and u_{av}^*. Therefore no mechanical sensors, such as tachometers or encoders, are needed for the experimental implementation of the ETEDPOF control. In fact, when it is applied to electromechanical systems, in general, such a passive control demands only the use of electric variables (see the applications previously mentioned in section I-C).
- The usage of the ETEDPOF methodology invariably results in linear, time-varying, state feedback controllers for trajectory tracking tasks, that achieve asymptotic stability [60], [61].
- The potential applications of this strategy is wide, since most of power electronics devices (such as DC/DC converters, DC/AC converters, and AC/DC converters) and interesting combinations of these devices with DC and AC motors are accurately described by the special "energy managing" structure (2). Moreover, nowadays, the ETEDPOF control law has applications in airships [64], mobile robotics [65], renewable energy systems [66], [68], and magnetorheological automotive suspensions [71].

Whereas the following is considered to be a limitation of the ETEDPOF control:

- When electrical abrupt changes, or mechanical load perturbations, are introduced in some parameters of the system the results show that the performance of the system in closed-loop is not robust. However, this could be overcome when the ETEDPOF control is modified as in [66] or when it is combined with algebraic estimation methods as in [14], [37], [67]–[69].

IV. GENERATION OF REFERENCE TRAJECTORIES VIA DIFFERENTIAL FLATNESS

The differential flatness property associated with (1) is used for generating the reference trajectories i^* and u_{av}^* that are required in (14). For this aim, firstly, it is shown that the full-bridge Buck inverter–DC motor system is controllable and, hence, differentially flat. Secondly, after differentially parameterizing all variables of the system in terms of the flat output, the required reference trajectories will be obtained. This, will allow the experimental implementation of the designed ETEDPOF control (14) for solving the trajectory tracking task on the full-bridge Buck inverter–DC motor system.

The average mathematical model of the full-bridge Buck inverter–DC motor system, given by (1), can be represented as:

$$\dot{x} = Ax + Bu_{av}, \tag{15}$$

where

$$A=\begin{bmatrix} 0 & -\frac{1}{L} & 0 & 0 \\ \frac{1}{C} & -\frac{1}{RC} & -\frac{1}{C} & 0 \\ 0 & \frac{1}{L_a} & -\frac{R_a}{L_a} & -\frac{k_e}{L_a} \\ 0 & 0 & \frac{k_m}{J} & -\frac{b}{J} \end{bmatrix}, \quad B=\begin{bmatrix} \frac{E}{L} \\ 0 \\ 0 \\ 0 \end{bmatrix}, \quad x=\begin{bmatrix} i \\ \upsilon \\ i_a \\ \omega \end{bmatrix}.$$

Based on [82], the controllability matrix $\mathcal{C}$ associated with (15) turns out to be,

$$\begin{aligned} \mathcal{C} &= [B \; AB \; A^2B \; A^3B] \\ &= \begin{bmatrix} \frac{E}{L} & 0 & -\frac{E}{L^2C} & \frac{E}{RL^2C^2} \\ 0 & \frac{E}{LC} & -\frac{E}{RLC^2} & -\frac{E(R^2LC+R^2L_aC-LL_a)}{R^2L^2L_aC^3} \\ 0 & 0 & \frac{E}{LL_aC} & -\frac{E(RR_aC+L_a)}{RLL_a^2C^2} \\ 0 & 0 & 0 & \frac{Ek_m}{JLL_aC} \end{bmatrix}. \end{aligned} \tag{16}$$

In this way, it is found that

$$\det \mathcal{C} = \frac{E^4k_m}{JL^4L_a^2C^3} \neq 0. \tag{17}$$

Thus, system (15) is controllable and, therefore, flat. From the latter and since $\mathcal{C}^{-1}$ exists, then it is possible to find the flat output of the system, y, from the following mathematical relation:

$$y = [0\;0\;0\;1]\mathcal{C}^{-1}x = \frac{JLL_aC}{Ek_m}\omega. \tag{18}$$

Consequently, and without loss of generality, the flat output is considered to be the angular velocity of the full-bridge Buck inverter–DC motor system, this is, $y = \omega$. In this way, variables i, υ, i_a, and the average control input u_{av}, all associated with (15), are determined by the following differential parameterization:

$$\begin{aligned} i =& \left(\frac{JL_aC}{k_m}\right)\omega^{(3)} + \left(\frac{bRL_aC + JRR_aC + JL_a}{k_mR}\right)\ddot{\omega} \\ &+ \left(\frac{bL_a + JR_a + JR + bRR_aC + k_ek_mRC}{k_mR}\right)\dot{\omega} \\ &+ \left(\frac{bR_a + k_ek_m + bR}{k_mR}\right)\omega, \end{aligned} \tag{19}$$

$$\upsilon = \frac{JL_a}{k_m}\ddot{\omega} + \left(\frac{bL_a + JR_a}{k_m}\right)\dot{\omega} + \left(\frac{bR_a}{k_m} + k_e\right)\omega, \tag{20}$$

$$i_a = \frac{J}{k_m}\dot{\omega} + \frac{b}{k_m}\omega, \tag{21}$$

and

$$\begin{aligned} u_{av} =& \left(\frac{JL_aLC}{Ek_m}\right)\omega^{(4)} \\ &+ \left(\frac{bRLL_aC + JRR_aLC + JLL_a}{Ek_mR}\right)\omega^{(3)} + \alpha\ddot{\omega} \\ &+ \left(\frac{bR_aL + k_ek_mL + bRL + bRL_a + JRR_a}{Ek_mR}\right)\dot{\omega} \\ &+ \left(\frac{bR_a + k_ek_m}{Ek_m}\right)\omega, \end{aligned} \tag{22}$$

with

$$\alpha = \frac{bLL_a + JR_aL + JRL + bRR_aLC + k_ek_mRLC + JRL_a}{Ek_mR}.$$

From the aforementioned, the reference trajectories i^*, υ^*, i_a^*, and u_{av}^* are obtained when a desired angular velocity profile ω^* is proposed and replaced into (19), (20), (21), and (22), respectively.

V. HARDWARE AND EXPERIMENTAL RESULTS IN CLOSED-LOOP

In order to validate the performance of the proposed ETEDPOF control, experimental tests are carried out on a built platform of the full-bridge Buck inverter–DC motor system. For this aim, a block diagram of the connections related to the system and the ETEDPOF control is firstly presented. Then, after executing the experimental tests associated with four different desired angular velocity profiles ω^* and by considering the system nominal parameters, given by (23) and (24), the obtained results are reported and commented. Later, an experimental assessment of the ETEDPOF control is realized when abrupt changes in the converter load R are introduced into the system. Lastly, the ETEDPOF control is experimentally compared with a PID control with the aim of verifying the dynamic response of the system in closed-loop.

A. DIAGRAM OF THE SYSTEM IN CLOSED-LOOP

Fig. 2 depicts the block diagram of the connections among the software (Matlab-Simulink), the hardware, and the system in closed-loop that has been used for the experimental tests.

The blocks composing the diagram of Fig. 2 are described below:

- *Desired trajectory and reference trajectories*. In this block, by using Matlab-Simulink, the desired angular velocity ω^*, and the reference trajectories i^*, υ^*, i_a^*, and u_{av}^* are programmed. These latter, are found through ω^* and the system differential parameterization given by (19)–(22).
- *ETEDPOF control*. The sensorless passivity-based control for solving the trajectory tracking task in the system, given by (14), is implemented in this block via Matlab-Simulink. The control gain parameter γ_1 was chosen to be:

  $$\gamma_1 = 0.003.$$

  While the measurement of the converter current, i, demanded by the proposed control is carried out via a Tektronix A622 current probe. Lastly, the reference trajectories i^* and u_{av}^* required in (14) are obtained from the block previously described.
- *Board and signal conditioning circuit*. This block shows the connections between the DS1104 board and the full-bridge Buck inverter–DC motor system. The realization of the discrete switching control (u) associated with the designed continuous control (u_{av}) is accomplished by

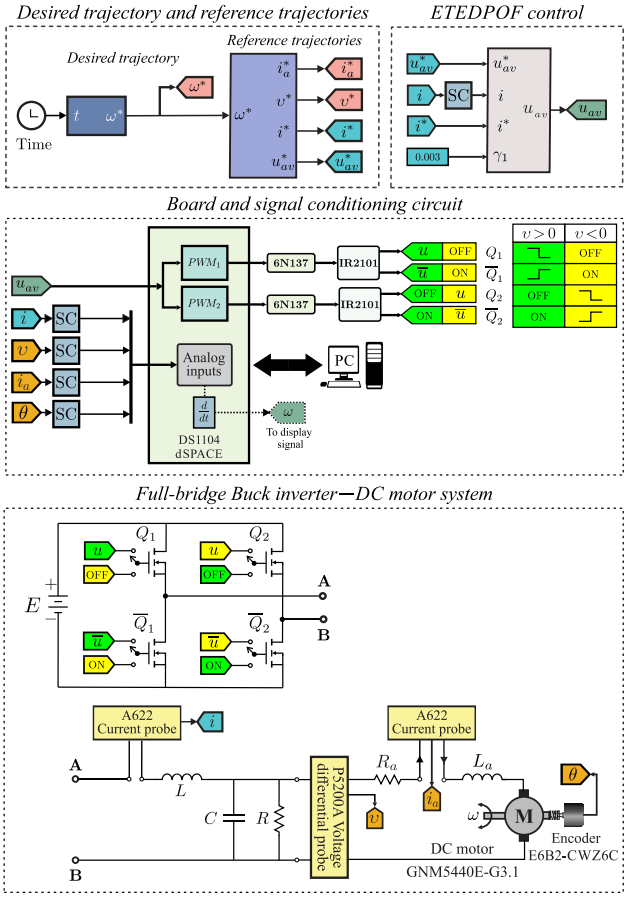

FIGURE 2. Software and hardware diagram of the full-bridge Buck inverter–DC motor system in closed-loop.

means of the PWM sub-blocks of the DS1104 board. Such a realization allows the correct activation of transistors Q_1, $\overline{Q}_1$, Q_2, and $\overline{Q}_2$ of the full-bridge inverter. Regarding the built circuit of the full-bridge inverter, four IRF640N MOSFET transistors and two IR2101 drivers are used. While the electric isolation between the DS1104 board and the power stage is achieved through optocouplers 6N137. On the other hand, currents (i and i_a), voltage (υ), and angular position (θ) are adapted by using signal conditioning (SC) blocks.

- *Full-bridge Buck inverter–DC motor system*. This block corresponds to the system under study. The values of parameters related to the full-bridge Buck inverter are the following:

$$E=32\text{ V},\ L=4.94\text{ mH},\ C=4.7\ \mu\text{F},\ R=48\ \Omega. \quad (23)$$

Regarding the DC motor, the values of its parameters correspond to those of the model ENGEL GNM5440E-G3.1 (24 V, 95 W) and are defined as,

$$\begin{aligned} L_a&=2.22\text{ mH}, & k_m&=120.1\times10^{-3}\ \tfrac{\text{N·m}}{\text{A}},\\ R_a&=0.965\ \Omega, & k_e&=120.1\times10^{-3}\ \tfrac{\text{V·s}}{\text{rad}},\\ J&=118.2\times10^{-3}\ \text{kg·m}^2, & b&=129.6\times10^{-3}\ \tfrac{\text{N·m·s}}{\text{rad}}. \end{aligned} \quad (24)$$

The measurements of i_a, υ, and θ were carried out with a Tektronix A622 current probe, a Tektronix P5200A voltage probe, and an Omron E6B2-CWZ6C incremental rotary encoder, respectively.

Lastly, a picture of the used hardware for starting up the full-bridge Buck inverter–DC motor system in closed-loop is shown in Fig. 3.

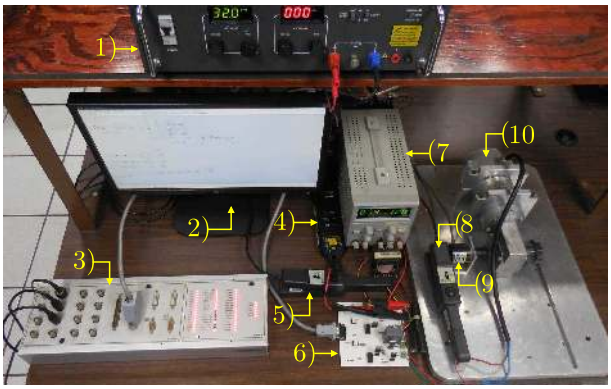

FIGURE 3. Picture of the used hardware for starting up the full-bridge Buck inverter–DC motor system in closed-loop: 1) Power supply E, 2) PC, 3) DS1104 board from dSPACE, 4) Tektronix P5200A voltage probe to measure υ, 5) Tektronix A622 current probe to measure i, 6) Full-bridge Buck inverter, 7) Power supply of the instrumentation stage, 8) Tektronix A622 current probe to measure i_a, 9) Omron E6B2-CWZ6C incremental rotary encoder to measure θ (and consequently, ω), and 10) DC motor.

B. EXPERIMENTAL RESULTS OF THE SYSTEM IN CLOSED-LOOP

With the aim of verifying the performance of the ETEDPOF control on the built system, in the following, the experimental results for four different desired angular velocity profiles are presented. Each plot shows first the results of the DC motor variables, i.e., ω and i_a and then the results associated with the full-bridge Buck inverter variables, i.e., i, υ, and u_{av}. In obtaining all the results of this subsection the nominal parameters of the full-bridge Buck inverter–DC motor system, previously defined in (23) and (24), have been used.

Experimental test 1

In this experiment, the proposed desired trajectory is of the Bézier type and is defined as,

$$\omega^*(t)=\overline{\omega}_i\left(t_i\right)+\left[\overline{\omega}_f(t_f)-\overline{\omega}_i\left(t_i\right)\right]\varphi\left(t,t_i,t_f\right), \quad (25)$$

where $\varphi\left(t,t_i,t_f\right)$ is given by

$$\varphi\left(t,t_i,t_f\right)=\begin{cases} 0 & t\le t_i,\\ \left(\frac{t-t_i}{t_f-t_i}\right)^5\times\left[252-1050\left(\frac{t-t_i}{t_f-t_i}\right)\right. & \\ \quad+1800\left(\frac{t-t_i}{t_f-t_i}\right)^2-1575\left(\frac{t-t_i}{t_f-t_i}\right)^3 & \\ \quad\left.+700\left(\frac{t-t_i}{t_f-t_i}\right)^4-126\left(\frac{t-t_i}{t_f-t_i}\right)^5\right] & \\ & t\in(t_i,t_f),\\ 1 & t\ge t_f. \end{cases}$$

With this proposal it is achieved that ω^* smoothly interpolates between $\overline{\omega}_i = -10$ $\frac{\text{rad}}{\text{s}}$ and $\overline{\omega}_f = 10$ $\frac{\text{rad}}{\text{s}}$ over the times $t_i = 4$ s and $t_f = 6$ s, respectively. The corresponding experimental results are depicted in Fig. 4.

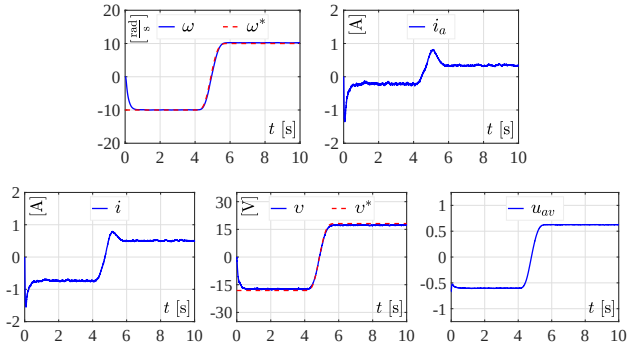

FIGURE 4. Results of the experimental implementation of control (14) on the full-bridge Buck inverter–DC motor system when the desired trajectory is of the Bézier type (25).

Experimental test 2

Now, with the intention of checking the performance of the control when periodic signals are considered as desired trajectories, in this second test the profile for ω^* is defined as a sinusoidal function given by,

$$\omega^*(t) = 10\,\sin(0.8\pi t). \tag{26}$$

The experimental results in closed-loop of this test are shown in Fig. 5.

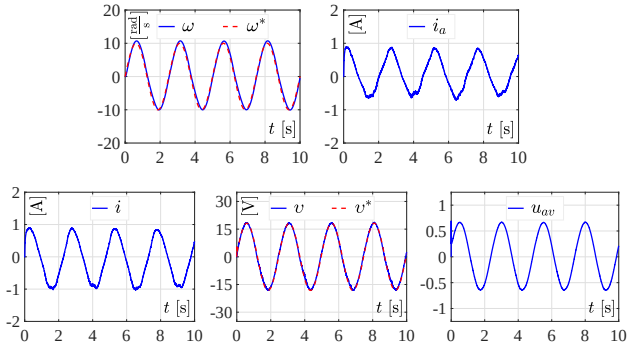

FIGURE 5. Experimental results of the full-bridge Buck inverter–DC motor system in closed-loop when the sinusoidal angular velocity profile (26) is considered.

Experimental test 3

The realization of the third experimental test takes into account the following desired angular velocity trajectory,

$$\omega^*(t) = 10\left(1 - e^{-2t^2}\right)\sin(0.8\pi t). \tag{27}$$

Thus, the corresponding experimental results are presented in Fig. 6.

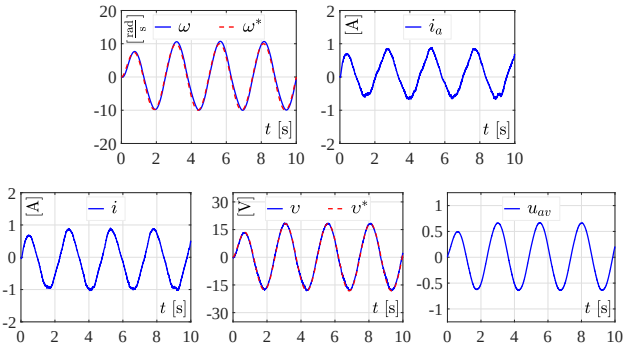

FIGURE 6. Experimental results in closed-loop when the desired angular velocity is defined by the sinusoidal with exponential amplitude type trajectory (27).

Experimental test 4

Lastly, the fourth experiment uses the desired trajectory profile defined in (28). While the obtained experimental results are depicted in Fig. 7.

$$\omega^*(t) = 10\,\sin(0.125\pi t^{\frac{3}{2}}). \tag{28}$$

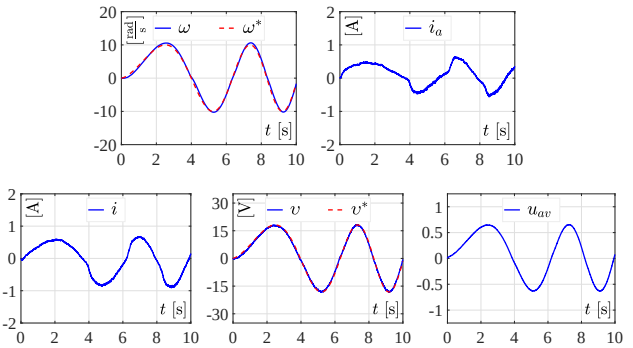

FIGURE 7. Experimental results associated with the implementation of the passivity-based control (14) when ω^* is considered to be the sinusoidal trajectory with time-varying frequency (28).

C. COMMENTS ON THE EXPERIMENTAL RESULTS

Based on the experimental results (see Figs. 4–7) it is concluded that the sensorless passivity-based control, for the angular velocity trajectory tracking task, in the full-bridge Buck inverter–DC motor system achieves the objective, i.e., $\omega \to \omega^*$.

Until now, the only experimental work related to the full-bridge Buck inverter–DC motor system, is the one where its mathematical model was developed and experimentally validated [59]. In the experimental tests reported in [59] the four desired trajectories ω^* used there were the same ones used in this paper, i.e., (25)–(28). Thus, in order to highlight the performance of the proposed ETEDPOF control (14), in the following, the similarity between ω versus ω^* and v versus v^* is quantified from the experimental results obtained in closed-loop (developed in this paper) and those

This article has been accepted for publication in a future issue of this journal, but has not been fully edited. Content may change prior to final publication. Citation information: DOI 10.1109/ACCESS.2021.3112575, IEEE Access

in open-loop (reported in [59]). This latter is realized with the intention of showing how the system is benefited from the designed ETEDPOF control, rather than for comparative purposes. Since, as it is well known, the closed-loop and the open-loop results cannot be compared; this is because in open-loop there is no feedback and, hence, no regulation is performed.

On the one hand, the closed-loop tracking errors associated with the experimental results of the angular velocity ($e_{\omega\, E_{cl}j}$) and the voltage ($e_{\upsilon\, E_{cl}j}$) are defined as:

$$\begin{aligned} e_{\omega\, E_{cl}j} &= \omega - \omega^*, \\ e_{\upsilon\, E_{cl}j} &= \upsilon - \upsilon^*, \end{aligned} \tag{29}$$

where subscript $E_{cl}j$, with $j \in \{1, 2, 3, 4\}$, indicates the experimental result in closed-loop from which the tracking error is obtained. On the other hand, the open-loop tracking errors associated with the experimental results for the angular velocity ($e_{\omega\, E_{ol}k}$) and for the voltage ($e_{\upsilon\, E_{ol}k}$) are defined as:

$$\begin{aligned} e_{\omega\, E_{ol}k} &= \omega - \omega^*, \\ e_{\upsilon\, E_{ol}k} &= \upsilon - \upsilon^*, \end{aligned} \tag{30}$$

where subscript $E_{ol}k$, with $k \in \{1, 2, 3, 4\}$, represents the experimental result in open-loop from which the tracking error is obtained [59].

Having defined the experimental closed-loop tracking errors in (29) and the experimental open-loop tracking errors in (30); the plots of the tracking errors for ω and υ, associated with the desired angular velocity profiles ω^* (25)–(28), are presented in Fig. 8. As can be observed in Figs. 8(a), 8(c), 8(e), and 8(g); it is clear that the closed-loop tracking errors for ω (i.e., $e_{\omega\, E_{cl}\{1,2,3,4\}}$) are smaller in magnitude than their corresponding open-loop tracking errors (i.e., $e_{\omega\, E_{ol}\{1,2,3,4\}}$). This, as previously mentioned, is due to in open-loop there is no feedback and consequently no regulation is performed; leading that the open-loop error be different to zero. And, in accordance with Figs. 8(b), 8(d), 8(f), and 8(h); a similar assess is obtained for the closed-loop tracking errors associated with υ (i.e., $e_{\upsilon\, E_{cl}\{1,2,3,4\}}$) in comparison with their corresponding open-loop tracking errors (i.e., $e_{\upsilon\, E_{ol}\{1,2,3,4\}}$). This, again, is due to in open-loop there is no feedback.

Meanwhile, note that the closed-loop tracking error plotted in Figs. 8(a) and 8(b) (see $e_{\omega\, E_{cl}1}$ and $e_{\upsilon\, E_{cl}1}$), and 8(g) and 8(h) (see $e_{\omega\, E_{cl}4}$ and $e_{\upsilon\, E_{cl}4}$) is smaller compared to the one plotted in Figs. 8(c) and 8(d) (see $e_{\omega\, E_{cl}2}$ and $e_{\upsilon\, E_{cl}2}$), and 8(e) and 8(f) (see $e_{\omega\, E_{cl}3}$ and $e_{\upsilon\, E_{cl}3}$). Such a behavior is due to the desired trajectories (25) and (28) have less sign changes compared to the desired trajectories (26) and (27), respectively.

From the aforementioned, it is concluded that the designed ETEDPOF control achieves the objective of trajectory tracking, i.e., $\omega \to \omega^*$, and also achieves that $\upsilon \to \upsilon^*$. Thus, validation of the performance associated with the designed sensorless passivity-based control, given by (14), for the angular velocity trajectory tracking task in the system, is satisfactory. However, in accordance with the limitation of the ETEDPOF strategy (previously mentioned in section III-C), such a control is not robust when some perturbations are considered into the system; this latter is verified in the following.

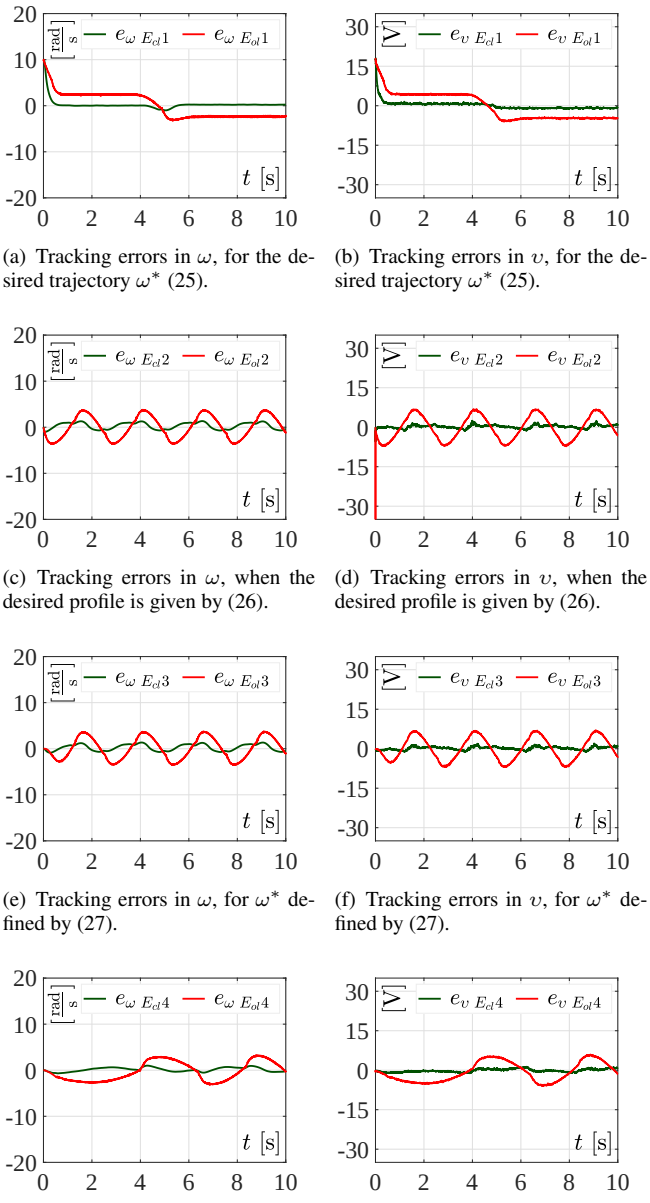

(a) Tracking errors in ω, for the desired trajectory ω^* (25).

(b) Tracking errors in υ, for the desired trajectory ω^* (25).

(c) Tracking errors in ω, when the desired profile is given by (26).

(d) Tracking errors in υ, when the desired profile is given by (26).

(e) Tracking errors in ω, for ω^* defined by (27).

(f) Tracking errors in υ, for ω^* defined by (27).

(g) Tracking errors in ω, for the desired trajectory (28).

(h) Tracking errors in υ, for desired trajectory (28).

FIGURE 8. Tracking errors of variables ω and υ of the full-bridge Buck inverter–DC motor system; associated with the four desired angular velocity profiles ω^* given by (25)–(28) and considering the system nominal parameters given by (23) and (24). Being $e_{\omega\, E_{cl}\{1,2,3,4\}}$ and $e_{\upsilon\, E_{cl}\{1,2,3,4\}}$ the obtained closed-loop tracking errors after implementing the proposed ETEDPOF control on the system. While $e_{\omega\, E_{ol}\{1,2,3,4\}}$ and $e_{\upsilon\, E_{ol}\{1,2,3,4\}}$ are related to the experimental open-loop tracking errors of the system.

Experimental test 5

This experimental test is performed when changes in R are introduced into the built experimental platform of the system.

Thus, with the aim of evaluating the performance of the system when abrupt variations are executed, the following change in R is proposed:

$$R_m = \begin{cases} R & 0 \text{ s} \leq t < 7.5 \text{ s}, \\ 30\%R & 7.5 \text{ s} \leq t \leq 10 \text{ s}. \end{cases} \tag{31}$$

The trajectory ω^* considered in *Experimental test 5* is defined in (25). The associated experimental results are presented in Fig. 9. Since the control based on ETEDPOF is not robust, a tracking error for v and ω will remain from $t \geq 7.5$ s to the end of the experiment. Thus, motivated by the experimental results when abrupt variations are executed into the system, the design of robust controls are considered as future work.

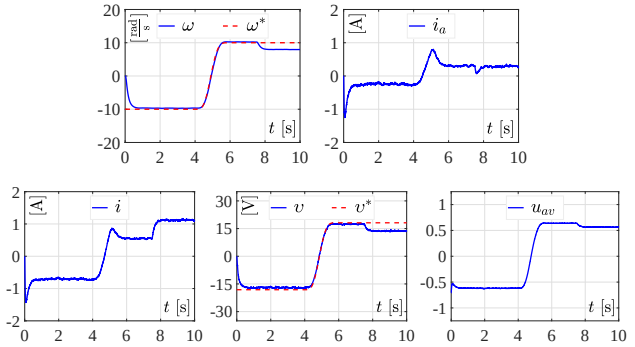

FIGURE 9. Results of the experimental implementation of control (14) on the full-bridge Buck inverter–DC motor system when ω^* is of the Bézier type (25) and the abrupt variations in R (31) are carried out.

Lastly, a visual comparison between the ETEDPOF control (14) and a PID control is carried out with the aim of verifying the dynamic response of the full-bridge Buck inverter–DC motor system in closed-loop. The experimental results are presented below.

Experimental test 6

In this experiment both, the ETEDPOF control and a PID control are experimentally implemented on the built platform of the system when the nominal parameters, defined in (23) and (24), are taken into account. The desired angular velocity trajectory to be followed by the motor shaft is proposed to be,

$$\omega^*(t) = \begin{cases} 0 & 0 \text{ s} \leq t < 3 \text{ s}, \\ 5 & 3 \text{ s} \leq t < 6 \text{ s}, \\ 10 & 6 \text{ s} \leq t < 9 \text{ s}, \\ 6 & 9 \text{ s} \leq t < 12 \text{ s}, \\ 0 & 12 \text{ s} \leq t < 15 \text{ s}, \\ -5 & 15 \text{ s} \leq t < 18 \text{ s}, \\ -10 & 18 \text{ s} \leq t < 21 \text{ s}, \\ -6 & 21 \text{ s} \leq t < 24 \text{ s}, \\ 0 & 24 \text{ s} \leq t < 27 \text{ s}. \end{cases} \tag{32}$$

The corresponding experimental results are depicted in Fig. 10. As can be observed in such a figure, the dynamic response of the system is apparently better when the PID control is used. However, it is also verified that the currents i_a and i and the voltage v, all of them associated with the ETEDPOF control, are smaller in magnitude than their corresponding ones related to the PID control, i.e., $i_{a_{PID}}$, i_{PID}, and v_{PID}, respectively. This latter implies that the PID control could compromise the integrity of the built platform, since the currents are bigger enough to damage the circuitry. Finally, note that the controls u_{av} and $u_{av_{PID}}$ never get saturated and the peaks of both signals are practically instantaneous.

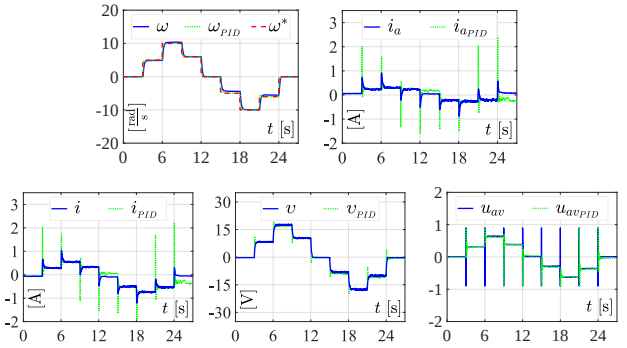

FIGURE 10. Experimental results of the ETEDPOF control (14) versus a PID control, both experimentally implemented on the full-bridge Buck inverter–DC motor system when ω^* is given by (32) and considering nominal parameters. Here, signals ω, i_a, i, v, and u_{av} are related to the ETEDPOF control. Whereas, signals ω_{PID}, $i_{a_{PID}}$, i_{PID}, v_{PID}, and $u_{av_{PID}}$ correspond to the PID control.

VI. CONCLUSIONS

A velocity-sensorless tracking control approach based on the exact tracking error dynamics passive output feedback (ETEDPOF) methodology for a new full-bridge Buck inverter–DC motor system was presented in this paper. With such a methodology, it is only required the measurement of current i and the knowledge of the reference trajectories i^* and u_{av}^* for solving the tracking related to ω. Therefore no mechanical sensors, such as tachometers and encoders, are needed for the implementation of the control. The nominal reference trajectories demanded by the ETEDPOF control are obtained by exploiting the differential flatness property of the mathematical model associated with the full-bridge Buck inverter–DC motor system. Regarding the implementation of the ETEDPOF control, its realization was executed by using Matlab-Simulink and the DS1104 board on a prototype of the system. According to the experimental results it is concluded that, in general, the trajectory tracking task is solved satisfactorily when system nominal parameters are considered. However, when abrupt variations in the system nominal parameters are introduced, ω and v no longer track to ω^* and v^*, respectively.

Finally, motivated by the obtained experimental results, in particular those in Fig. 9, the design of a robust control that takes into account abrupt perturbations in parameters of the system is considered as future work. Also, applications in AC motors, mechatronic systems, robotic arms, wheeled mobile robots, underactuated mechanical systems, and renewable energy are considered as future work.

REFERENCES

[1] J. F. Gieras, *Permanent Magnet Motor Technology: Design and Applications,* 3rd ed. Boca Raton, FL, USA: CRC Press, 2010.

[2] S. E. Lyshevski, *Electromechanical Systems, Electric Machines, and Applied Mechatronics.* Boca Raton, FL, USA: CRC Press, 1999.

[3] M. A. Ahmad, R. M. T. Raja-Ismail, and M. S. Ramli, "Control strategy of Buck converter driven DC motor: A comparative assessment," *Australian J. Basic Appl. Sci.*, vol. 4, no. 10, pp. 4893–4903, Oct. 2010. [Online]. Available: http://www.ajbasweb.com/old/ajbas/2010/4893-4903.pdf

[4] O. Bingöl and S. Paçaci, "A virtual laboratory for neural network controlled DC motors based on a DC-DC Buck converter," *Int. J. Eng. Educ.*, vol. 28, no. 3, pp. 713–723, 2012.

[5] H. Sira-Ramírez and M. A. Oliver-Salazar, "On the robust control of Buck-converter DC-motor combinations," *IEEE Trans. Power Electron.*, vol. 28, no. 8, pp. 3912–3922, Aug. 2013, doi: 10.1109/TPEL.2012.2227806.

[6] F. E. Hoyos, A. Rincón, J. A. Taborda, N. Toro, and F. Angulo, "Adaptive quasi-sliding mode control for permanent magnet DC motor," *Math. Probl. Eng.*, vol. 2013, Nov. 2013, Art. ID 693685. [Online]. Available: https://doi.org/10.1155/2013/693685

[7] F. E. Hoyos-Velasco, J. E. Candelo-Becerra, and A. Rincón-Santamaría, "Dynamic analysis of a permanent magnet DC motor using a Buck converter controlled by ZAD-FPIC", *Energies*, vol. 11, no. 12, Dec. 2018, Art. no. 3388. [Online]. Available: https://doi.org/10.3390/en11123388

[8] F. E. Hoyos, J. E. Candelo-Becerra, and C. I. Hoyos-Velasco, "Application of zero average dynamics and fixed point induction control techniques to control the speed of a DC motor with a Buck converter," *Appl. Sci.*, vol. 10, no. 5, Mar. 2020, Art. no. 1807. [Online]. Available: https://doi.org/10.3390/app10051807

[9] F. E. Hoyos, J. E. Candelo-Becerra, and A. Rincón, "Zero average dynamic controller for speed control of DC motor," *Appl. Sci.*, vol. 11, no. 12, Jun. 2021, Art. no. 5608. [Online]. Available: https://doi.org/10.3390/app11125608

[10] R. Silva-Ortigoza, J. R. García-Sánchez, J. M. Alba-Martínez, V. M. Hernández-Guzmán, M. Marcelino-Aranda, H. Taud, and R. Bautista-Quintero, "Two-stage control design of a Buck converter/DC motor system without velocity measurements via a Σ–Δ-modulator," *Math. Probl. Eng.*, vol. 2013, Jun. 2013, Art. ID 929316. [Online]. Available: https://doi.org/10.1155/2013/929316

[11] R. Silva-Ortigoza, C. Márquez-Sánchez, F. Carrizosa-Corral, M. Antonio-Cruz, J. M. Alba-Martínez, and G. Saldaña-González, "Hierarchical velocity control based on differential flatness for a DC/DC Buck converter-DC motor system," *Math. Probl. Eng.*, vol. 2014, Apr. 2014, Art. ID 912815. [Online]. Available: https://doi.org/10.1155/2014/912815

[12] F. Wei, P. Yang, and W. Li, "Robust adaptive control of DC motor system fed by Buck converter," *Int. J. Control Autom.*, vol. 7, no. 10, pp. 179–190, Oct. 2014. [Online]. Available: http://dx.doi.org/10.14257/ijca.2014.7.10.17

[13] R. Silva-Ortigoza, V. M. Hernández-Guzmán, M. Antonio-Cruz, and D. Muñoz-Carrillo, "DC/DC Buck power converter as a smooth starter for a DC motor based on a hierarchical control," *IEEE Trans. Power Electron.*, vol. 30, no. 2, pp. 1076–1084, Feb. 2015. [Online]. Available: https://ieeexplore.ieee.org/document/6767144

[14] G. K. Srinivasan and H. T. Srinivasan, "Sensorless load torque estimation and passivity based control of Buck converter fed DC motor," *Sci. World J.*, vol. 2015, Mar. 2015, Art. ID 132843. [Online]. Available: https://doi.org/10.1155/2015/132843

[15] V. M. Hernández-Guzmán, R. Silva-Ortigoza, and D. Muñoz-Carrillo, "Velocity control of a brushed DC-motor driven by a DC to DC Buck power converter," *Int. J. Innov. Comput. Inf. Control*, vol. 11, no. 2, pp. 509–521, Apr. 2015. [Online]. Available: http://www.ijicic.org/ijicic-110209.pdf

[16] S. Khubalkar, A. Chopade, A. Junghare, M. Aware, and S. Das, "Design and realization of stand-alone digital fractional order PID controller for Buck converter fed DC motor," *Circuits Syst. Signal Process.*, vol. 35, no. 6, pp. 2189–2211. Jun. 2016, doi: 10.1007/s00034-016-0262-2.

[17] G. Rigatos, P. Siano, P. Wira, and M. Sayed-Mouchaweh, "Control of DC-DC converter and DC motor dynamics using differential flatness theory," *Intell. Ind. Syst.*, vol. 2, no. 4, pp. 371–380, Dec. 2016. [Online]. Available: https://link.springer.com/article/10.1007/s40903-016-0061-x

[18] T. K. Nizami, A. Chakravarty, and C. Mahanta, "Design and implementation of a neuro-adaptive backstepping controller for Buck converter fed PMDC-motor," *Control Engineering Practice*, vol. 58, pp. 78–87, Jan. 2017, doi: 10.1016/j.conengprac.2016.10.002.

[19] G. Rigatos, P. Siano, S. Ademi, and P. Wira "Flatness-based control of DC-DC converters implemented in successive loops," *Electric Power Components and Systems*, vol. 46, no. 6, pp. 673–687, 2018, doi: 10.1080/15325008.2018.1464612.

[20] S. W. Khubalkar, A. S. Junghare, M. V. Aware, A. S. Chopade, and S. Das, "Demonstrative fractional order – PID controller based DC motor drive on digital platform," *ISA Transactions*, vol. 82, pp. 79–93, Nov. 2018, doi: 10.1016/j.isatra.2017.08.019.

[21] J. Yang, H. Wu, L. Hu, and S. Li, "Robust predictive speed regulation of converter-driven DC motors via a discrete-time reduced-order GPIO," *IEEE Trans. Ind. Electron.*, vol. 66, no. 10, pp. 7893–7903, Oct. 2019, doi: 10.1109/TIE.2018.2878119.

[22] M. I. F. M. Hanif, M. H. Suid, and M. A. Ahmad, "A piecewise affine PI controller for Buck converter generated DC motor," *International Journal of Power Electronics and Drive Systems*, vol. 10, no. 3, pp. 1419–1426, Sep. 2019. [Online]. Available: http://ijpeds.iaescore.com/index.php/IJPEDS/article/view/19852

[23] M. G. Kazemi and M. Montazeri, "Fault detection of continuous time linear switched systems using combination of bond graph method and switching observer," *ISA Transactions*, vol. 94, pp. 338–351, Nov. 2019, doi: 10.1016/j.isatra.2019.04.023.

[24] G. Rigatos, P. Siano, and M. Sayed-Mouchaweh, "Adaptive neurofuzzy H-infinity control of DC–DC voltage converters," *Neural Computing and Applications*, vol. 32, no. 7, pp. 2507–2520, Apr. 2020, doi: 10.1007/s00521-019-04394-4.

[25] A. Rauf, S. Li, R. Madonski, and J. Yang, "Continuous dynamic sliding mode control of converter-fed DC motor system with high order mismatched disturbance compensation," *Transactions of the Institute of Measurement and Control*, vol. 42, no. 14, pp. 2812–2821, Oct. 2020, doi: 10.1177/0142331220933415.

[26] G. K. Srinivasan, H. T. Srinivasan, and M. Rivera, "Sensitivity analysis of exact tracking error dynamics passive output control for a flat/partially flat converter systems," *Electronics*, vol. 9, no. 11, Nov. 2020, Art. no. 1942. [Online]. Available: https://doi.org/10.3390/electronics9111942

[27] M. R. Stanković, R. Madonski, S. Shao, and D. Mikluc, "On dealing with harmonic uncertainties in the class of active disturbance rejection controllers," *International Journal of Control*, 2020. Published online: 11 Mar. 2020, doi: 10.1080/00207179.2020.1736639.

[28] R. Madonski, K. Łakomy, M. Stankovic, S. Shao, J. Yang, and S. Li, "Robust converter-fed motor control based on active rejection of multiple disturbances," *Control Engineering Practice*, vol. 107, Feb. 2021, Art. no. 104696, doi: 10.1016/j.conengprac.2020.104696.

[29] M. D. Patil, K. Vadirajacharya, and S. W. Khubalkar, "Design and tuning of digital fractional-order PID controller for permanent magnet DC motor," *IETE Journal of Research*, 2021. Published online: 28 Jun. 2021, doi: 10.1080/03772063.2021.1942243.

[30] A. Rauf, M. Zafran, A. Khan, and A. R. Tariq, "Finite-time nonsingular terminal sliding mode control of converter-driven DC motor system subject to unmatched disturbances," *International Transactions on Electrical Energy Systems*, 2021, Art. no. e13070. Published online: 21 Aug. 2021, doi:10.1002/2050-7038.13070.

[31] R. Silva-Ortigoza, J. N. Alba-Juárez, J. R. García-Sánchez, M. Antonio-Cruz, V. M. Hernández-Guzmán, and H. Taud, "Modeling and experimental validation of a bidirectional DC/DC Buck power electronic converter–DC motor system," *IEEE Latin Amer. Trans.*, vol. 15, no. 6, pp. 1043–1051, Jun. 2017, doi: 10.1109/TLA.2017.7932691.

[32] R. Silva-Ortigoza, J. N. Alba-Juárez, J. R. García-Sánchez, V. M. Hernández-Guzmán, C. Y. Sosa-Cervantes, and H. Taud, "A sensorless passivity-based control for the DC/DC Buck converter–inverter–DC motor system," *IEEE Latin Amer. Trans.*, vol. 14, no. 10, pp. 4227–4234, Oct. 2016, doi: 10.1109/TLA.2016.7786298.

[33] E. Hernández-Márquez, J. R. García-Sánchez, R. Silva-Ortigoza, M. Antonio-Cruz, V. M. Hernández-Guzmán, H. Taud, and M. Marcelino-Aranda, "Bidirectional tracking robust controls for a DC/DC Buck converter-DC motor system," *Complexity*, vol. 2018, Aug. 2018, Art. ID 1260743. [Online]. Available: https://doi.org/10.1155/2018/1260743

[34] X. Chi, S. Quan, J. Chen, Y.-X. Wang, and H. He, "Proton exchange membrane fuel cell-powered bidirectional DC motor control based on adaptive sliding-mode technique with neural network estimation," *International Journal Hydrogen Energy*, vol. 45, no. 39, pp. 20282–20292, Aug. 2020, doi: 10.1016/j.ijhydene.2019.12.224.

[35] A. A. A. Ismail and A. Elnady, "Advanced drive system for DC motor using multilevel DC/DC Buck converter circuit," *IEEE Ac-*

cess, vol. 7, pp. 54167–54178, May 2019. [Online]. Available: https://ieeexplore.ieee.org/document/8695686

[36] E. Guerrero, E. Guzmán, J. Linares, A. Martínez, and G. Guerrero, "FPGA-based active disturbance rejection velocity control for a parallel DC/DC Buck converter-DC motor system," *IET Power Electron.*, vol.13, no. 2, pp. 356–367, Feb. 2020. [Online]. Available: https://doi.org/10.1049/iet-pel.2019.0832

[37] J. Linares-Flores, J. Reger, and H. Sira-Ramírez, "Load torque estimation and passivity-based control of a Boost-converter/DC-motor combination," *IEEE Trans. Control Syst. Technol.*, vol. 18, no. 6, pp. 1398–1405, Nov. 2010, doi: 10.1109/TCST.2009.2037809.

[38] A. T. Alexandridis and G. C. Konstantopoulos, "Modified PI speed controllers for series-excited DC motors fed by DC/DC Boost converters," *Control Engineering Practice*, vol. 23, pp. 14–21, Feb. 2014, doi: 10.1016/j.conengprac.2013.10.009.

[39] S. Malek, "A new nonlinear controller for DC-DC Boost converter fed DC motor," *Int. J. Power Electron.*, vol. 7, nos. 1–2, pp. 54–71, 2015, doi: 10.1504/IJPELEC.2015.071199.

[40] G. C. Konstantopoulos and A. T. Alexandridis, "Enhanced control design of simple DC-DC Boost converter-driven DC motors: Analysis and implementation," *Electric Power Components and Systems*, vol. 43, no. 17, pp. 1946–1957, 2015, doi: 10.1080/15325008.2015.1070383.

[41] P. Mishra, A. Banerjee, M. Ghosh, and C. B. Baladhandautham, "Digital pulse width modulation sampling effect embodied steady-state time-domain modeling of a Boost converter driven permanent magnet DC brushed motor," *International Transactions on Electrical Energy Systems*, vol. 31, no. 8, Aug. 2021, Art. no. e12970, doi: 10.1002/2050-7038.12970.

[42] V. H. García-Rodríguez, R. Silva-Ortigoza, E. Hernández-Márquez, J. R. García-Sánchez, and H. Taud, "DC/DC Boost converter-inverter as driver for a DC motor: Modeling and experimental verification," *Energies*, vol. 11, no. 8, Aug. 2018, Art. no. 2044. [Online]. Available: https://doi.org/10.3390/en11082044

[43] R. Silva-Ortigoza, V. H. García-Rodríguez, E. Hernández-Márquez, M. Ponce, J. R. García-Sánchez, J. N. Alba-Juárez, G. Silva-Ortigoza, and J. H. Pérez-Cruz, "A trajectory tracking control for a Boost converter-inverter-DC motor combination," *IEEE Latin Amer. Trans.*, vol. 16, no. 4, pp. 1008–1014, Apr. 2018, doi: 10.1109/TLA.2018.8362130.

[44] J. R. García-Sánchez, E. Hernández-Márquez, J. Ramírez-Morales, M. Marciano-Melchor, M. Marcelino-Aranda, H. Taud, and R. Silva-Ortigoza, "A robust differential flatness-based tracking control for the "MIMO DC/DC Boost converter-inverter-DC motor" system: Experimental results," *IEEE Access*, vol. 7, pp. 84497–84505, Jul. 2019. [Online]. Available: https://ieeexplore.ieee.org/abstract/document/8740891

[45] Y. Sönmez, M. Dursun, U. Güvenç, and C. Yilmaz, "Start up current control of Buck-Boost convertor-fed serial DC motor," *Pamukkale Univ. J. Eng. Sci.*, vol. 15, no. 2, pp. 278–283, 2009.

[46] J. Linares-Flores, J. L. Barahona-Avalos, H. Sira-Ramírez, and M. A. Contreras-Ordaz, "Robust passivity-based control of a Buck-Boost-converter/DC-motor system: An active disturbance rejection approach," *IEEE Trans. Ind. Appl.*, vol. 48, no. 6, pp. 2362–2371, Nov./Dec. 2012, doi: 10.1109/TIA.2012.2227098.

[47] E. Hernández-Márquez, R. Silva-Ortigoza, J. R. García-Sánchez, V. H. García-Rodríguez, and J. N. Alba-Juárez, "A new 'DC/DC Buck-Boost converter–DC motor' system: Modeling and experimental validation," *IEEE Latin Amer. Trans.*, vol. 15, no. 11, pp. 2043–2049, Nov. 2017, doi: 10.1109/TLA.2017.8070406.

[48] E. Hernández-Márquez, R. Silva-Ortigoza, J. R. García-Sánchez, M. Marcelino-Aranda, and G. Saldaña-González, "A DC/DC Buck-Boost converter–inverter–DC motor system: Sensorless passivity-based control," *IEEE Access*, vol. 6, pp. 31486–31492, Jun. 2018. [Online]. Available: https://ieeexplore.ieee.org/document/8382160

[49] E. Hernández-Márquez, C. A. Avila-Rea, J. R. García-Sánchez, R. Silva-Ortigoza, G. Silva-Ortigoza, H. Taud, and M. Marcelino-Aranda, "Robust tracking controller for a DC/DC Buck-Boost converter–inverter–DC motor system," *Energies*, vol. 11, no. 10, Oct. 2018, Art. no. 2500. [Online]. Available: https://doi.org/10.3390/en11102500

[50] M. R Ghazali, M. A. Ahmad, and R. M. T. Raja-Ismail, "Adaptive safe experimentation dynamics for data-driven neuroendocrine-PID control of MIMO systems," *IETE J. Res.*, 2019. Published online: 17 Sep. 2019, doi:10.1080/03772063.2019.1656556.

[51] J. Linares-Flores, H. Sira-Ramírez, E. F. Cuevas-López, and M. A. Contreras-Ordaz, "Sensorless passivity based control of a DC motor via a solar powered Sepic converter-full bridge combination," *J. Power Electron.*, vol. 11, no. 5, pp. 743–750, Sep. 2011. [Online]. Available: https://jpels.org/digital-library/archives

[52] G. K. Srinivasan, H. T. Srinivasan, and M. Rivera, "Low-cost implementation of passivity-based control and estimation of load torque for a Luo converter with dynamic load," *Electronics*, vol. 9, no. 11, Nov. 2020, Art. no. 1914. [Online]. Available: https://doi.org/10.3390/electronics9111914

[53] M. H. Arshad and M. A. Abido, "Hierarchical control of DC motor coupled with Cuk converter combining differential flatness and sliding mode control," *Arabian Journal for Science and Engineering*, 2021. Published online: 19 Jan. 2021, doi: 10.1007/s13369-020-05305-9.

[54] K. Erenturk, "Hybrid control of a mechatronic system: Fuzzy logic and grey system modeling approach," *IEEE/ASME Transactions on Mechatronics*, vol. 12, no. 6, pp. 703–710, Dec. 2007, doi: 10.1109/TMECH.2007.910118.

[55] K. V. R. Swathi and G. V. Nagesh-Kumar, "Design of intelligent controller for reduction of chattering phenomenon in robotic arm: A rapid prototyping," *Comput. Electr. Eng.*, vol. 74, pp. 483–497, Mar. 2019, doi: 10.1016/j.compeleceng.2017.12.010.

[56] R. Silva-Ortigoza, J. R. García-Sánchez, V. M. Hernández-Guzmán, C. Márquez-Sánchez, and M. Marcelino-Aranda, "Trajectory tracking control for a differential drive wheeled mobile robot considering the dynamics related to the actuators and power stage," *IEEE Latin Amer. Trans.*, vol. 14, no. 2, pp. 657–664, Feb. 2016, doi: 10.1109/TLA.2016.7437207.

[57] J. R. García-Sánchez, S. Tavera-Mosqueda, R. Silva-Ortigoza, V. M. Hernández-Guzmán, J. Sandoval-Gutiérrez, M. Marcelino-Aranda, H. Taud, and M. Marciano-Melchor, "Robust switched tracking control for wheeled mobile robots considering the actuators and drivers," *Sensors*, vol. 18, no. 12, Dec. 2018, Art. no. 4316. [Online]. Available: https://doi.org/10.3390/s18124316

[58] J. R. García-Sánchez, S. Tavera-Mosqueda, R. Silva-Ortigoza, V. M. Hernández-Guzmán, M. Marciano-Melchor, J. de J. Rubio, M. Ponce-Silva, M. Hernández-Bolaños, and J. Martínez-Martínez, "A novel dynamic three-level tracking controller for mobile robots considering actuators and power stage subsystems: Experimental assessment," *Sensors*, vol. 20, no. 17, Sep. 2020, Art. no. 4959. [Online]. Available: https://doi.org/10.3390/s20174959

[59] E. Hernández-Márquez, C. A. Avila-Rea, J. R. García-Sánchez, R. Silva-Ortigoza, M. Marciano-Melchor, M. Marcelino-Aranda, A. Roldán-Caballero, and C. Márquez-Sánchez, "New "full-bridge Buck inverter-DC motor" system: Steady-state and dynamic analysis and experimental validation," *Electronics*, vol. 8, no. 11, Nov. 2019, Art. no.1216. [Online]. Available: https://doi.org/10.3390/electronics8111216

[60] H. Sira-Ramírez, "Are nonlinear controllers really necessary in power electronics devices?" in *Proc. 11th Eur. Conf. Power Electron. Appl.*, Dresden, Germany, Sep. 2005, pp. 1–10, doi: 10.1109/EPE.2005.219747.

[61] H. Sira-Ramírez and R. Silva-Ortigoza, *Control Design Techniques in Power Electronics Devices*. London, U.K.: Springer-Verlag, 2006.

[62] M. Flota, R. Alvarez-Salas, H. Rodríguez-Cortés, and C. Nuñez, "Nonlinear partial state feedback controller for a single phase active rectifier," in *Proc. 5th International Conference on Electrical Engineering, Computing Science and Automatic Control*, Mexico City, Mexico, Nov. 2008, pp. 20–25, doi: 10.1109/ICEEE.2008.4723377.

[63] A. Gensior, H. Sira-Ramírez, J. Rudolph, and H. Güldner, "On some nonlinear current controllers for three-phase Boost rectifiers," *IEEE Trans. Ind. Electron.*, vol. 56, no. 2, pp. 360–370, Feb. 2009, doi: 10.1109/TIE.2008.2003370.

[64] G. Murguía-Rendon, H. Rodríguez-Cortés, and M. Velasco-Villa, "Trajectory tracking control for the planar dynamics of a thrust vectored airship," in *Proc. 52nd IEEE International Midwest Symposium on Circuits and Systems*, Cancun, Mexico, Aug. 2009, pp. 329–332, doi: 10.1109/MWSCAS.2009.5236089.

[65] M. Velasco-Villa, H. Rodríguez-Cortés, I. Estrada-Sanchez, H. Sira-Ramírez, and J. A. Vázquez, "Dynamic trajectory-tracking control of an omnidirectional mobile robot based on a passive approach," in *Advances in Robot Manipulators*, E. Hall, Ed., Rijeka, Croatia: InTech, 2010, ch. 15, pp. 299–314. [Online]. Available: https://www.intechopen.com/chapters/11044

[66] H. Sira-Ramírez, M. A. Oliver-Salazar, and J. Leyva-Ramos, "Voltage regulation of a fuel cell-Boost converter system: A proportional integral exact tracking error dynamics passive output feedback control approach," in *Proc. 2012 American Control Conference*, Montréal, Canada, Jun. 2012, pp. 2153–2158, doi: 10.1109/ACC.2012.6314843.

[67] H. Sira-Ramírez, C. García-Rodríguez, J. Cortés-Romero, and A. Luviano-

Juárez, *Algebraic Identification and Estimation Methods in Feedback Control Systems*. Chennai, India: John Wiley & Sons, 2014.

[68] J. Linares-Flores, J. F. Guerrero-Castellanos, R. Lescas-Hernández, A. Hernández-Méndez, and R. Vázquez-Perales, "Angular speed control of an induction motor via a solar powered Boost converter-voltage source inverter combination," *Energy*, vol. 166, pp. 326–334, Jan. 2019, doi: 10.1016/j.energy.2018.10.024.

[69] J. A. Juárez-Abad, A. P. Sandoval-García, J. Linares-Flores, J. F. Guerrero-Castellanos, P. Bañuelos-Sánchez, and M. A. Contreras-Ordaz, "FPGA implementation of passivity-based control and output load algebraic estimation for transformerless multilevel active rectifier," *IEEE Transactions on Industrial Informatics*, vol. 15, no. 4, pp. 1877–1889, Apr. 2019, doi: 10.1109/TII.2018.2865445.

[70] J. Linares-Flores, A. Hernández-Méndez, J. J. Vásquez-Sanjuan, J. F. Guerrero-Castellanos, and G. Curiel-Olivares, "Robust sensorless low-speed trajectory tracking for a permanent magnet synchronous motor: An extended state observer based backstepping control approach," *Advanced Control for Applications*, vol. 2, no. 3, Sep. 2020, Art. no. e49. [Online]. Available: https://doi.org/10.1002/adc2.49

[71] K. H. Floreán-Aquino, M. Arias-Montiel, J. Linares-Flores, J. G. Mendoza-Larios, and Á. Cabrera-Amado, "Modern semi-active control schemes for a suspension with MR actuator for vibration attenuation," *Actuators*, vol. 10, no. 2, Feb. 2021, Art. no. 22. [Online]. Available: https://doi.org/10.3390/act10020022

[72] V. M. Hernández-Guzmán, R. Silva-Ortigoza, S. Tavera-Mosqueda, M. Marcelino-Aranda, and M. Marciano-Melchor, "Path-tracking of a WMR fed by inverter-DC/DC Buck power electronic converter systems," *Sensors*, vol. 20, no. 22, Nov. 2020, Art. no. 6522. [Online]. Available: https://doi.org/10.3390/s20226522

[73] V. M. Hernández-Guzmán, R. Silva-Ortigoza, and J. Orrante-Sakanassi, "Velocity control of a PMSM fed by an inverter-DC/DC Buck power electronic converter," *IEEE Access*, vol. 8, pp. 69448–69460, Apr. 2020. [Online]. Available: https://ieeexplore.ieee.org/document/9061159

[74] V. M. Hernández-Guzmán, "Velocity control of an induction motor fed by an inverter-DC/DC Buck power electronic converter," *International Journal of Control*, 2021. Published online: 28 Jan. 2021, doi: 10.1080/00207179.2021.1876925.

[75] S. Zaare and M. R. Soltanpour, "The position control of the ball and beam system using state-disturbance observe-based adaptive fuzzy sliding mode control in presence of matched and mismatched uncertainties," *Mechanical Systems and Signal Processing*, vol. 150, Mar. 2021, Art. no. 107243, doi: 10.1016/j.ymssp.2020.107243.

[76] L. Zhang and R. Dixon, "Robust nonminimal state feedback control for a Furuta pendulum with parametric modeling errors," *IEEE Trans. Ind. Electron.*, vol. 68, no. 8, pp. 7341–7349, Aug. 2021, doi: 10.1109/TIE.2020.3001811.

[77] W. Acuña-Bravo, A. G. Molano-Jiménez, and E. Canuto, "Embedded model control for underactuated systems: An application to Furuta pendulum," *Control Engineering Practice*, vol. 113, Aug. 2021, Art. no. 104854, doi: 10.1016/j.conengprac.2021.104854.

[78] J. Sandoval, J. Moyrón, R. Kelly, V. Santibáñez, and J. Moreno-Valenzuela, "Energy regulation for a torque-driven vertical inertia wheel pendulum," *Control Engineering Practice*, vol. 115, Oct. 2021, Art. no. 104909, doi: 10.1016/j.conengprac.2021.104909.

[79] J. Sandoval, R. Kelly, and V. Santibáñez, "An output feedback position/speed regulator for a torque–driven inertia wheel pendulum," *Int. J. Control Automat. Syst.*, 2021. Published online: 30 Mar. 2021, doi: 10.1007/s12555-020-0744-7.

[80] V. M. Hernández-Guzmán, V. Santibáñez, and G. Herrera, "Control of rigid robots equipped with brushed DC-motors as actuators," *Int. J. Control Automat. Syst.*, vol. 5, no. 6, pp. 718–724, Dec. 2007. [Online]. Available: http://www.ijcas.org

[81] D. R. Merkin, *Introduction to the Theory of Stability.* New York, NY, USA: Springer-Verlag, 1997.

[82] H. Sira-Ramírez and S. K. Agrawal, *Differentially Flat Systems*. New York, NY, USA: Marcel Dekker, 2004.